NIH Public Access
Author Manuscript
Biochemistry. Author manuscript; available in PMC 2012 July 12.

Published in final edited form as:
Biochemistry. 2011 July 12; 50(27): 6093–6101. doi:10.1021/bi200288c.

Acrylodan smooth muscle tropomyosin reports differences in effects of troponin and caldesmon in the transition from the active state to the inactive state†

Joseph M. Chalovich[*,#], **Evan Lutz**[#], **Tamatha Baxley**[#], and **Mechthild M. Schroeter**[Ξ]

[#] Brody School of Medicine at East Carolina University;5E-122 Brody Medical Sciences Building; Greenville, NC 27834

[Ξ] Institute of Vegetative Physiology, University of Cologne, Robert-Koch-Str. 39, D-50931, Cologne, Germany

Abstract

Changes in the orientation of tropomyosin on actin are important for the regulation of striated muscle contraction and could also be important for smooth muscle regulation. We showed earlier that acrylodan-labeled skeletal muscle tropomyosin reports the kinetics of the reversible transitions among the active, intermediate and inactive states when S11 is rapidly detached from actin-tropomyosin. We now show that acrylodan-labeled smooth muscle tropomyosin reports similar transitions among states of actin-tropomyosin. When S1 was rapidly detached from actin-smooth muscle tropomyosin there was a rapid decrease in acrylodan-tropomyosin fluorescence as the intermediate state became populated. The rate constant for this process was >600/sec at temperatures near 5° C. In the presence of skeletal troponin and EGTA, the decrease in fluorescence was followed by a redevelopment of fluorescence as the inactive state became populated. The apparent rate constant for the fluorescence increase was 14/sec at 5° C. Substituting smooth muscle caldesmon for skeletal muscle troponin produced a similar decrease and re-increase in fluorescence but the apparent rate constant for the increase was >10 times that observed with troponin. Furthermore, the fluorescence increase was correlated with an increase in caldesmon attachment as S1-ATP dissociated. Although the measured rate constant appeared to reflect the rate limiting transition for inactivation it is unclear if the fluorescence change resulted from caldesmon binding, tropomyosin movement over actin or both.

Actin-based regulation of striated mammalian muscle contraction is dependent on the position of tropomyosin on actin. Troponin stabilizes tropomyosin in the inactive state at low free Ca^{2+} concentrations. There is little or no activation of the ATPase activity of myosin S1 when actin filaments are in that state. Calcium binding to troponin releases tropomyosin from the inhibitory position so that it rapidly samples the active state (greatest activation of ATPase activity), the intermediate state and the inactive state. The intermediate state allows modest stimulation of myosin ATPase activity and is the most highly populated state at this condition. Binding of rigor myosin S1 to actin stabilizes the active state (1), (2) where tropomyosin occupies a unique position on actin (3).

†Funded by National Institutes of Health Grant # AR035216 to J.M.C.

[1]Abbreviations: EGTA, ethylene glycol-bis(β-aminoethyl ether)-N,N,N′,N′-tetraacetic acid; MOPS, 3-(N-morpholino)propanesulfonic acid; NBD,7-chloro-4-nitrobenzo-2-oxa-1,3-diazole; NEM, N-ethylmaleimide; regulated actin, actin-tropomyosin-troponin; S1, myosin subfragment 1.

[*]Corresponding Author: Fax: 252-744-3383, Phone: 252-744-2973, chalovichj@ecu.edu.

NIH-PA Author Manuscript
NIH-PA Author Manuscript
NIH-PA Author Manuscript

NIH-PA Author Manuscript

NIH-PA Author Manuscript

NIH-PA Author Manuscript

The inhibitory component of troponin, TnI, competes for binding with myosin-ATP in the absence of tropomyosin. However, that competition of binding is largely eliminated in the presence of tropomyosin (4). The actin-troponin-tropomyosin complex is stable; troponin is not displaced even by the high affinity binding of myosin in the presence of ADP.

Smooth muscle also contains an actin-linked regulatory system (5) consisting of tropomyosin and the actin binding protein caldesmon (6). Smooth muscle tropomyosin differs from skeletal tropomyosin in several ways. Skeletal tropomyosin inhibits actin activation of myosin S1-ATPase activity over a wide range of conditions. Smooth muscle tropomyosin produces a steep increase in ATPase rate with increasing ionic strength with a crossover point from inhibition to activation near 0.05 M ionic strength (7). The head to tail interactions of smooth tropomyosin are stronger than those of the skeletal variety (8). There is a greater degree of stabilization of the active state of actin-tropomyosin per myosin S1 bound to actin for the smooth muscle variety of tropomyosin (9). Skeletal muscle tropomyosin is a mixture of αα homodimers and αβ heterodimers; smooth muscle tropomyosin appears to be 100% αβ heterodimer (10).

Caldesmon is an actin binding protein (6) that appears to participate in regulation of non-muscle and smooth muscle contraction (11), (12). Caldesmon inhibits both actin activation of the rate of ATP hydrolysis by myosin and also myosin S1 binding to actin. Tropomyosin enhances the ability of caldesmon to inhibit actin activated ATPase activity (13), (14), (15). Caldesmon differs from troponin in that it remains competitive with S1-ATP binding in the presence of tropomyosin (16), (17), (18). Our data suggest that this inhibition of binding is biologically relevant (16), (17), (18), (19) and proportional to the extent of inhibition of ATPase activity (20). Other studies suggest that the inhibition of S1-ATP binding occurs at higher concentrations of caldesmon than necessary to inhibit the rate of actin-activated ATP hydrolysis (21).

Because tropomyosin is a component of actin filaments of both smooth and striated muscle it is interesting to know the extent to which the inhibitory activity of caldesmon can be attributed to movement of tropomyosin on actin. Pyrene labeled smooth muscle tropomyosin bound to actin undergoes a change in fluorescence in the presence of caldesmon that has been attributed to movement of tropomyosin into an inhibitory state (22). However, image reconstructions of actin filaments containing smooth muscle tropomyosin and an actin binding caldesmon fragment show that tropomyosin does not occupy the same inhibitory position that is stabilized by troponin in the absence of calcium (23). We reexamined the question of tropomyosin movement using an acrylodan probe on smooth muscle tropomyosin that has certain advantages over pyrene tropomyosin for measuring transitions of actin-tropomyosin-troponin (24).

Skeletal muscle troponin stabilizes the inactive state of skeletal tropomyosin-actin in the absence of calcium. We found that skeletal muscle troponin had a similar effect with smooth muscle acrylodan-tropomyosin bound to actin. The transition from the active state to the intermediate state occurred with a very rapid decrease in fluorescence followed by a slower increase in fluorescence as the inactive state became populated.

A similar pattern was observed with caldesmon except that the fluorescence increase was faster than with troponin and of smaller amplitude. The fluorescence increase was correlated with caldesmon binding to actin-tropomyosin following S1-ATP detachment. With both troponin and caldesmon the slow increase in acrylodan-tropomyosin fluorescence appeared to reflect the rate constant for transition to the inactive state. In the case of troponin the change in acrylodan-tropomyosin fluorescence was attributed to movement of tropomyosin. In the case of caldesmon, the change in fluorescence was due either to caldesmon binding or

NIH-PA Author Manuscript

NIH-PA Author Manuscript

NIH-PA Author Manuscript

to some subsequent process. Other results confirm the importance of competition of binding between caldesmon and myosin S1.

We previously used the notation 1(0) for the inactive state, 1(2) for the intermediate state and 2(0), 2(1) or 2(2) for the active state of regulated actin (25). The first digit indicates the activity: 1 for low activity and 2 for high activity. The second digit, shown here in parentheses, is the number of bound calcium ions per troponin. The more recent nomenclature, blocked (inactive), closed (intermediate) and open (active), assumes a model of regulation that involves blocking myosin binding sites on actin (26). Because of different views of regulation of striated muscle (27) and uncertainties in regulation of smooth muscle addressed in the present paper we use the model-independent descriptors based on the measured levels of ATPase activity: inactive, intermediate and active.

Experimental Procedures

Proteins

Actin (28), troponin (29) and myosin (30) were prepared from rabbit back muscle. Myosin S1 was prepared by digestion of myosin with chymotrypsin (31). Smooth muscle tropomyosin was prepared from turkey gizzards (32). Caldesmon was isolated from turkey gizzards by two methods (32), (15).

Protein concentrations were determined using the following extinction coefficients: ($\varepsilon^{0.1\%}$) for 280 nm: actin, 1.15; myosin S1, 0.75; smooth muscle tropomyosin, 0.22; caldesmon, 0.39 and troponin, 0.45. The molecular weights of the proteins were assumed to be: actin, 42,000; myosin S1, 120,000; tropomyosin, 68,000; caldesmon, 87,000; troponin, 69,000.

Acrylodan-labeled and pyrene-labeled smooth muscle tropomyosin were prepared as described for skeletal muscle tropomyosin (24) using a 10:1 molar ratio of acrylodan or N-(1-pyrene)iodoacetamide to tropomyosin. These conditions gave >70% labeling using extinction coefficients of 22,000 $M^{-1}cm^{-1}$ at 344 nm for pyrene and 14,400 $M^{-1}cm^{-1}$ at 372 nm for acrylodan (33). Caldesmon was labeled with NBD by reaction with N-((2-(iodoacetoxy)ethyl)-N-methyl)-amino-7-nitrobenz-2-oxa-1,3-diazole as described earlier (34). Concentrations of fluorescently labeled proteins were determined by the Lowry method.

Actin-Activated Myosin S1 ATPase Rates

ATPase rates were measured to determine the effect of labeling on the function of tropomyosin and to set limits on the distribution of states of regulated actin. ATPase rates were measured by the rate of liberation of $^{32}P_i$ from γ^{32}P-ATP (35). Assays were measured at 25° C in reactions containing 0.3 μM S1, 10 μM actin, 3.5 μM tropomyosin, 4.3 μM troponin or 0.5–7.5 μM caldesmon in a buffer containing 2 mM ATP, 4.8 mM $MgCl_2$, 35.8 mM NaCl, 10 mM MOPS, 0.5 mM dithiothreitol, 1 mM EGTA or 0.5 mM $CaCl_2$, pH 7.

In some cases S1 treated with N-ethylmaleimide (NEM-S1) was used to stabilize actin filaments in the active state in the presence of ATP (36). N-ethylmaleimide labeled myosin S1 was prepared by reacting myosin 4 mg/ml S1 with a 15-fold molar excess of N-ethylmaleimide at 25°C for 30 min in a buffer containing 100 mM KCl, 50 mM Tris(hydroxyethyl)aminomethane-HCl, pH 8.0. After exhaustive dialysis the modified S1 was clarified by centrifugation. The concentration of actin was increased by an amount equal to the added NEM-S1 concentration to maintain a constant free actin concentration (36).

NIH-PA Author Manuscript

NIH-PA Author Manuscript

NIH-PA Author Manuscript

Fluorescence Time Courses

Rapid kinetic measurements were made with a SF20 sequential mixing stopped flow spectrometer (Applied Photophysics Ltd, Leatherhead, Surrey, United Kingdom) equipped with circulating water temperature regulation. The excitation wavelength was fixed with a monochrometer using a slit width of either 0.5 or 1 mm. Acrylodan was excited with light at a wavelength of 391 nm and fluorescence was measured through a Schott GG 455 (Duryea, PA) high pass filter with a 455 nm midpoint. Light scattering measurements were generally made simultaneously with acrylodan fluorescence measurements with a low pass filter that blocks light above 430 nm and with a 392 midpoint. NBD fluorescence was monitored by excitation at 492 nm and emission was measured with an Oriel #51284 high pass filter (Edmund Optics, Barrington, NJ) having a cut on midpoint at 517 nm. Most data curves are averages of 4 measurements.

S1-ATP dissociation studies

The active state of actin-tropomyosin was stabilized with bound S1. Upon rapidly adding ATP, the S1-ATP complex dissociated allowing tropomyosin to return to its normal state. In the absence of other bound proteins, ATP caused a transition from the active state to a mixture of states that is enriched in the intermediate or inactive states depending on the source of actin and tropomyosin (37). In the presence of skeletal troponin and absence of calcium, tropomyosin moved from the active state to the intermediate state. Experiments in the presence of caldesmon were done to determine if the inactive state was stabilized as in the troponin case.

Two models were used to simulate the experiments. A, X and I are the active, intermediate and inactive states of actin-tropomyosin, M is myosin S1, and C is caldesmon.

$$\text{Model A: ATP+M} - \text{A} \underset{k_{2A}}{\overset{k_{1A}}{\rightleftarrows}} \text{ATP} - \text{M} - \text{A} \underset{k_{4A}}{\overset{k_{3A}}{\rightleftarrows}} \text{ATP} - \text{M+A}; \quad \text{A} \underset{k_{6A}}{\overset{k_{5A}}{\rightleftarrows}} \text{X} \underset{k_{8A}}{\overset{k_{7A}}{\rightleftarrows}} \text{I}$$

$$\text{Model B:} \quad \text{X+C} \underset{k_{2B}}{\overset{k_{1B}}{\rightleftarrows}} \text{XC} \underset{k_{4B}}{\overset{k_{3B}}{\rightleftarrows}} \text{IC}$$

Model B has caldesmon bound only to the intermediate and inactive states. This assumption was made because the rate of transition from the active state to the intermediate state is much faster than the rate of caldesmon binding.

Simulations of the kinetics were done only in those cases where the rate of ATP binding was much faster than the succeeding reactions so that the rate constants defining ATP binding could be ignored. The differential equations used to simulate the ATP dissociation studies (Model A) were shown earlier (24). S1-ATP detachment was simulated by examining the change of ATP-M-A with time. Transitions from the active state to the inactive state were simulated by examining the time courses of A, X and I multiplied by their relative fluorescence intensities: F_A*A + F_X*X + F_I*I. The relative fluorescence of state A, F_A, was set to 1. The value of F_I was determined experimentally to be 0.95. The value of F_X was permitted to float in simulations.

Time courses were also evaluated by fitting exponential models to the data. Such analyses give combinations of rate constants or apparent rate constants indicated here by the symbol k_{app}. Values of k_{app} for the fast fluorescence decrease were slower than the calculated rate constant k_{3A} in cases where the rapid fluorescence decrease had a decay rate ≥ that for the preceding light scattering change. Values of k_{3A} were adjusted so that both the light scattering and fluorescence curves were fit by the model. These values are prone to error

NIH-PA Author Manuscript

NIH-PA Author Manuscript

NIH-PA Author Manuscript

because rates of light scattering and the rapid fluorescence decrease were near the limit of time resolution of the measurements.

RESULTS

Regulation of ATPase activity

Smooth muscle tropomyosin that was unmodified or labeled with either acrylodan or pyrene probes increased the degree of actin activation of S1 ATPase activity (Figure 1A). However, the magnitude of this increase was reduced by labeling. In the absence of caldesmon the pyrene label reduced the ATPase rate by 42% but acrylodan labeling reduced the rate by only 23%. Both types of labeled tropomyosin were regulated by caldesmon to give similar minimum activities. Furthermore, the concentration of caldesmon required to give 50% inhibition was about the same for all types of tropomyosin.

Figures 1B and 1C show that acrylodan smooth tropomyosin was also well regulated by skeletal troponin. Figure 1B shows that acrylodan smooth tropomyosin increased the rate by 1.5 fold compared to actin alone. In contrast the rate with skeletal tropomyosin was only 32% of the rate with actin alone under these conditions (not shown). Skeletal troponin gave 15-fold calcium regulation to actin-acrylodan smooth tropomyosin. Under the same conditions skeletal troponin gave 21-fold calcium regulation with unlabeled skeletal tropomyosin (not shown). ATPase rates with acrylodan smooth tropomyosin and skeletal troponin were about 3-fold faster in EGTA and 2-fold faster in Ca^{2+} than with skeletal tropomyosin.

Acrylodan labeled smooth tropomyosin supported potentiation (1) of ATPase activity by high affinity myosin complexes. That is, NEM-labeled S1 binding to actin-tropomyosin-troponin increased the ATPase above the Ca^{2+}-activated rate by about 2-fold (Figure 1C). The ratio of rates at the fully active state to the inactive state was 30-fold. Thin filaments containing actin and acrylodan labeled smooth muscle tropomyosin were capable of existing in the inactive (troponin and EGTA), intermediate (no addition) or fully active (NEM-S1) states.

Acrylodan Tropomyosin Transitions

Acrylodan tropomyosin fluorescence was dependent on the state of activation of actin-tropomyosin. In the absence of added effectors actin-tropomyosin exists primarily in an intermediate state (Figure 2A, lower solid line). Both the active state (stabilized with S1, vertical bars) and the inactive state (stabilized with calcium-free troponin, horizontal bars) had high fluorescence relative to the intermediate state. The low fluorescence of the intermediate state was seen previously with acrylodan labeled skeletal tropomyosin (24). The mean relative fluorescence values from 490–540 nm were 1.0 in the presence of S1 and 0.95 in the presence of troponin and EGTA. The observed relative fluorescence in the absence of S1 and troponin was 0.85. Because the latter is a mixture of states this represents an upper limit for the relative fluorescence of the intermediate state. If the intermediate state constituted 65% of the total in the calcium saturated condition, the fluorescence of the intermediate would be about 0.77. Figure 2B shows that caldesmon (horizontal bars) increased the fluorescence of actin-acrylodan tropomyosin (lower solid curve) but to a smaller extent than did troponin. The addition of S1 to actin-acrylodan tropomyosin-caldesmon increased the fluorescence to its maximum level (vertical bars).

Figure 2C confirms that the calcium binding to actin-acrylodan tropomyosin-troponin enriched the population of the low fluorescence state. A rapid decrease in Ca^{2+} increased the fluorescence (curve 1) whereas a rapid rise in Ca^{2+} reduced the fluorescence (curve 2).

NIH-PA Author Manuscript

NIH-PA Author Manuscript

NIH-PA Author Manuscript

Rate of Acrylodan Tropomyosin Transition in the absence of inhibitory proteins

Kinetics of transitions from the active state were measured by using ATP to rapidly displace bound S1 from actin-tropomyosin allowing actin-tropomyosin to return from the fully active state to either the intermediate or inactive state. In the absence of an inhibitory protein the intermediate state is favored. Figure 3 shows that following dissociation by ATP there was a rapid reduction in light scattering as S1-ATP detached from actin. This was followed by a decrease in acrylodan-tropomyosin fluorescence as the actin-tropomyosin moved largely to the intermediate state.

At high ATP concentrations the rate of S1 detachment could only be measured at low temperatures. Fitting model A to the light scattering traces gave rates of S1 detachment in the order of 700/sec (+/− 110/sec, n=6) at 5° C. An analysis of the fluorescence transition by Model A was possible if the equilibrium constant for the transition between the intermediate and inactive states was set so that the inactive state was not significantly populated. If the rate of S1 detachment was restricted to values obtained from light scattering measurements the rate constant for the transition between the active and intermediate states must be greater 600/sec (+/− 88/sec, n=16).

Rate of transition in the presence of troponin and absence of calcium

Figure 4 shows the effects of rapid detachment of S1-ATP in the presence of skeletal troponin and EGTA. The rapid decrease in fluorescence resulting from the loss of the active state was followed by a slower increase in fluorescence as the inactive state became populated. The minimum in fluorescence occurred at the point where the intermediate state was most heavily populated. This result is consistent with Figure 2 and is similar to the behavior of acrylodan labeled skeletal muscle tropomyosin (24).

The rate constant for detachment of S1-ATP, k_{3A} was >630/sec. The transition between the intermediate and inactive states was often too fast to observe. Simulations with model A indicated that this could occur if the rate constant from the active state to the intermediate state, k_{5A}, was >1200/sec.

The rate constants for the transition from the intermediate state to the inactive state were relatively insensitive to the values of the rate constants used for fitting S1-ATP detachment and the transition from the active to the intermediate state. The rate constants were independent both of the fraction of actin initially bound to S1 over the observed range from 0.25 to 1.0 and over the concentration range of ATP from 0.5 to 2 mM. Rate constants (k_7 + k_8) were estimated using model A to be 10/sec (2.7° C), 13/sec (3.5° C), 14/sec (5° C) and 19/sec (8.2° C).

Rate of transition in the presence of caldesmon

Acrylodan tropomyosin fluorescence responses to rapid S1-ATP detachment in the presence of caldesmon were similar to those observed in the presence of troponin (Figure 5A). The rapid fluorescence decrease due to the transition to the intermediate was difficult to observe and appeared to be limited by the rate of S1-ATP dissociation from actin. The amplitude of the signal for the S1-ATP dissociation experiment was dependent on the amount of S1 initially bound to actin-tropomyosin. The amplitude was 50% of its maximum value when the actin was approximately 40% saturated with S1 (data not shown). The maximum signal occurred when there was nearly a 1:1 mixture of actin and S1. When the S1 concentration was reduced to give 25% saturation of the actin the initial downward phase of fluorescence was not seen but the fluorescence increase occurred normally (inset to Figure 5A). Transition rates between the intermediate and inactive states tended to be faster than seen at

NIH-PA Author Manuscript

NIH-PA Author Manuscript

NIH-PA Author Manuscript

the same concentration of troponin. Rate constants for the transition to the inactive state were independent of the fraction of actin initially bound to S1 over the range 0.25 to 1.0.

The concentrations of ATP used to dissociate S1 from actin were varied from 0.005 to 2 mM to determine if the observed transition rate constants were independent of the ATP concentration. Figure 5B shows examples of traces at 0.5 and 0.05 mM ATP. Reductions in ATP concentration led to slower detachment of S1, slower transition to the intermediate state and reduced amplitude of the fluorescence recovery (Figure 5B). At concentrations of ATP less than or equal to 0.05 mM the fluorescence increases were too small to be analyzed.

Figure 5C shows the ATP dependencies of S1-ATP detachment and the subsequent fluorescence decrease. The apparent rate constants for S1-ATP dissociation (scattering) were similar to those for rapid acrylodan fluorescence decreases at all ATP concentrations examined. This differed from the case with skeletal tropomyosin and troponin where the light scattering change was faster than the fluorescence change (24). These results confirmed that the observed transition to the intermediate state was limited by the rate of S1-ATP detachment. Estimates of the rate of transition to the inactive state were relatively insensitive to the ATP concentration at or above 0.5 mM ATP where the amplitude was relatively large.

Because S1 and caldesmon compete for binding to actin it was possible that caldesmon bound to actin-tropomyosin only after S1-ATP dissociated. Several experiments were done to determine if the slower redevelopment of fluorescence resulted from caldesmon binding.

NBD-labeled caldesmon monitors caldesmon binding directly to actin. Figure 6A compares the results of rapid S1-ATP dissociation from actin containing bound NBD-caldesmon and unlabeled tropomyosin with a binding study in which NBD caldesmon was mixed directly with actin-tropomyosin. The S1-ATP dissociation experiment, shown as vertical bars was indistinguishable from the NBD-caldesmon binding experiment (dots). Both curves are well described by a theoretical curve for NBD-caldesmon binding to actin in a 2-step process (Model B). Fitting these results did not require an assumption of tropomyosin movement of the kind observed with the troponin study.

Figure 6B shows that when caldesmon was rapidly added to a mixture of actin and acrylodan labeled tropomyosin there was an increase in fluorescence that was similar to that observed in the S1-ATP dissociation experiments. The amplitude of the transients increased with increasing caldesmon concentrations indicating that saturation of the signal required rather high caldesmon concentrations. The transitions were simulated with Model B. While this model does not incorporate the cooperative features of caldesmon binding as did our earlier analysis (34) it is useful for comparison with the S1-ATP dissociation studies.

S1-ATP dissociation experiments were also done with variable caldesmon concentrations at low ionic strength where the amount of bound caldesmon could be estimated from past measurements (15), (20). Four such curves are shown in Figure 7A. These data were analyzed in a model-independent manner by fitting a biexponential function to the rising part of the curves. The major process of the biexponential function was the more rapid transition. Both the apparent rate constant (Figure 7B) and the amplitude (inset to Figure 7B) increased with the free caldesmon concentration in a hyperbolic manner. The curves for k_{app} and the amplitude were fitted globally with the same value of the apparent dissociation constant. This result shows that the fluorescence increase is associated with high levels of caldesmon binding to actin-tropomyosin.

We examined the possibility that the observed fluorescence change reflected caldesmon binding directly to acrylodan labeled tropomyosin. Mixing unlabeled caldesmon directly with acrylodan labeled tropomyosin did produce an increase in fluorescence with a similar

NIH-PA Author Manuscript

NIH-PA Author Manuscript

NIH-PA Author Manuscript

rate constant to that obtained in the presence of actin (data not shown). The magnitude of that fluorescence change was 33–50% of that for binding to actin-tropomyosin. Therefore, the area of tropomyosin near the site of attachment of the fluorescent probes was sensitive to caldesmon.

DISCUSSION

Acrylodan labeled smooth muscle tropomyosin provides the capability of measuring the kinetics of the transitions of actin-tropomyosin among the active, intermediate and inactive states. As was seen earlier with acrylodan labeled skeletal tropomyosin, the intermediate state has the lowest fluorescence intensity. Thus the direction of the fluorescence change helped to identify the transition that was being observed. The acrylodan probe is superior to the pyrene probe in its ability to monitor the transition between the intermediate and inactive states. The acrylodan probe could be used at lower temperature than the pyrene probe for monitoring tropomyosin transitions (24). Because of the rapidity of the transitions it was important in the present case to work at low temperatures. Furthermore labeling with acrylodan does not require the formation of alpha-alpha homodimers of smooth muscle tropomyosin. This is an advantage because smooth muscle tropomyosin consists almost exclusively of alpha-beta heterodimers (10).

The present study showed another advantage of the acrylodan probe. Labeling with acrylodan was less deleterious to the regulatory response of smooth muscle tropomyosin than labeling with pyrene. Actin filaments containing acrylodan labeled smooth muscle tropomyosin and skeletal muscle troponin were regulated normally by calcium and exhibited “potentiation” at high concentrations of the activator, NEM-S1.

Upon rapid detachment of S1-ATP from actin-tropomyosin-troponin there was a rapid decrease in acrylodan tropomyosin fluorescence followed by a slower increase. The pattern observed was similar to that reported with skeletal tropomyosin (24) and indicates that acrylodan labeled smooth muscle tropomyosin monitors transitions from the active to the intermediate to the inactive states. The transition from the active state to the intermediate state was limited by the rate of S1-ATP release; simulations with Model A required that the rate constant for the A to X transition were faster than the rate constant for S1-ATP release. That differs from the situation with skeletal tropomyosin where the fluorescence transition was slower than S1-ATP detachment under some conditions (24).

The use of skeletal troponin demonstrated the utility of acrylodan labeled smooth muscle tropomyosin so that it could be used in context with its biological partner, caldesmon. At physiological ionic strength, smooth muscle tropomyosin increases the actin activated ATPase activity of S1 above that seen with actin alone. Caldesmon appears to reverse that activating effect of tropomyosin. In addition, caldesmon inhibits the binding of S1-ATP to actin and to actin-tropomyosin (17) (18). There is disagreement over the relative importance of these effects in the presence of tropomyosin. Ansari et al. studied the effect of caldesmon on the actin filaments containing pyrene labeled smooth muscle tropomyosin (22). They interpreted caldesmon induced changes in tropomyosin pyrene excimer fluorescence as movement of tropomyosin over actin and concluded that caldesmon functions in the same manner as troponin does. Because of advantages afforded by the acrylodan probe we sought verification of that finding. Additionally, we wished to determine the effect of caldesmon on the kinetics of transitions among actin states.

Equilibrium binding of caldesmon to acrylodan-tropomyosin-actin increased the acrylodan fluorescence. S1-ATP dissociation studies in the presence of caldesmon also produced transitions that were similar to those obtained with troponin. However control experiments

NIH-PA Author Manuscript

NIH-PA Author Manuscript

NIH-PA Author Manuscript

revealed a fundamental difference between the effects of troponin and caldesmon. Caldesmon bound to actin-tropomyosin only after S1-ATP dissociated from actin. This was verified with NBD-caldesmon binding to actin-tropomyosin in Fig 6. The fluorescence of NBD-caldesmon monitors actin binding (17) and the fluorescence occurred only after S1-ATP detached. Furthermore, the time courses for NBD-caldesmon binding were similar to acrylodan-tropomyosin fluorescence changes. That is, changes in NBD-caldesmon and acrylodan-tropomyosin were limited by the same process. The slow increase in fluorescence, in the presence of caldesmon, does reflect inhibition of ATPase activity but does not indicate whether that inhibition results from competitive binding with S1 or movement of tropomyosin.

Ansari et al. suggested that if caldesmon and troponin produced the same change in tropomyosin then the addition of caldesmon to actin-tropomyosin-troponin would cause no additional change in fluorescence (22). We found it impossible to interpret such addition experiments because in our hands troponin displaced NBD-labeled caldesmon from actin-tropomyosin (data not shown).

In an attempt to distinguish caldesmon binding from a subsequent conformational change in tropomyosin we examined S1-ATP dissociation experiments at varied caldesmon concentrations under conditions where the affinity of caldesmon to actin-tropomyosin is known. Both the rate and amplitude of the observed acrylodan tropomyosin transition increased as the caldesmon concentration was increased. Saturation of changes in amplitude and rate occurred under moderate caldesmon concentrations. We did not observe evidence to support a population of high affinity binding sites that were correlated with the movement of tropomyosin as has been proposed (21).

There is a temptation to directly apply experimental approaches that have been used for troponin to investigate the mechanism of caldesmon function. However, unlike troponin, the complex of caldesmon with actin and tropomyosin is unstable in the presence of myosin. Interpretation of studies involving caldesmon, myosin, and actin requires knowledge of the amount of caldesmon and S1 bound to actin at each point in an experiment. Because caldesmon binds to myosin (38), as well as to actin, it is also necessary to determine how the amount of caldesmon and myosin bound **directly** to actin change during the course of the experiment.

There is another clear distinction between troponin and caldesmon that makes interpretation of fluorescence changes by the same mechanism tenuous. Caldesmon and troponin are known to produce distinct changes in the orientation of tropomyosin on actin. Skeletal tropomyosin exists primarily in the intermediate state or position “C” near the junction of the inner and outer domains. Calcium-free troponin moved skeletal tropomyosin to the inactive state or position “B” away from the groove of the actin helix (3), (39). Smooth muscle tropomyosin was found to be located on the inner edge of the outer domain of actin in position “B” or inhibited state (37). Addition of sufficient C-terminal fragment of caldesmon to have 1 fragment bound per 3 actin monomers moved smooth tropomyosin toward the inner domain of actin or the open state. The authors concluded that caldesmon and troponin act by different structural mechanisms (23).

Acrylodan labeled smooth muscle tropomyosin monitors the state of activity of actin filaments regardless of whether the activity is changed by troponin or caldesmon. In both cases the state of intermediate activity is a low fluorescence state. In the case of troponin the fluorescence changes reflect the transition of tropomyosin among different positions on actin. In the case of caldesmon the fluorescence changes could be due to caldesmon binding to actin-tropomyosin, to tropomyosin movement or both. If a component of the inhibition by

NIH-PA Author Manuscript

NIH-PA Author Manuscript

NIH-PA Author Manuscript

caldesmon involves movement of tropomyosin it does so by moving tropomyosin into a different position than is stabilized by troponin. *The* mechanism of tropomyosin movement would involve caldesmon binding followed by tropomyosin movement or coupled to tropomyosin movement. The rate constant for tropomyosin movement would have to be greater than 14x that observed with troponin indicating a different kind of transition.

Although probes on tropomyosin cannot by themselves distinguish among models of caldesmon function the concentration dependencies of such changes are informative. We argued earlier that the major effect of caldesmon is to inhibit binding of S1-ATP to actin and to actin-tropomyosin (17), (17), (18). We observed a single class of moderate affinity caldesmon binding sites on actin (20). Displacement of S1-ATP correlated with filling those sites. Others argued that filling high affinity sites on actin is correlated with inhibition of ATPase activity by a tropomyosin-mediated effect (21) that involves the rate of product release (40). They suggested that inhibition of S1-ATP binding occurs as a set of low affinity sites that saturates with 1 caldesmon bound per actin protomer. However the concentration dependencies of apparent rate constants and fluorescence amplitudes for S1-ATP dissociation experiments in the presence of caldesmon shown in Figure 7 are consistent with a single class of moderate affinity sites as we observed earlier (41).

Acknowledgments

The authors wish to acknowledge the able assistance of Mr. Jayson Varughese in running some control studies for this work.

References

1. Murray JM, Knox MK, Trueblood CE, Weber A. Potentiated state of the tropomyosin actin filament and nucleotide-containing myosin subfragment 1. Biochemistry. 1982; 21:906–915. [PubMed: 6462176]
2. Greene LE, Eisenberg E. Cooperative binding of myosin subfragment-1 to the actin-troponin-tropomyosin complex. Proc Natl Acad Sci USA. 1980; 77:2616–2620. [PubMed: 6930656]
3. Poole KJV, Lorenz M, Evans G, Rosenbaum G, Pirani A, Craig R, Tobacman LS, Lehman W, Holmes KC. A comparison of muscle thin filament models obtained from electron microscopy reconstructions and low-angle X-ray fibre diagrams from non-overlap muscle. J Struct Biol. 2006; 155:273–284. [PubMed: 16793285]
4. Resetar AM, Stephens JM, Chalovich JM. Troponin-tropomyosin: an allosteric switch or a steric blocker? Biophys J. 2002; 83:1039–1049. [PubMed: 12124285]
5. Marston SB, Smith CWJ. The thin filaments of smooth muscles. J Muscle Res Cell Motil. 1985; 6:669–708. [PubMed: 3937845]
6. Sobue K, Muramoto Y, Fujita M, Kakiuchi S. Purification of a calmodulin-binding protein from chicken gizzard that interacts with F-actin. Proc Natl Acad Sci USA. 1981; 78:5652–5655. [PubMed: 6946503]
7. Williams DL, Greene LE, Eisenberg E. Comparison of effects of smooth and skeletal muscle tropomyosins in interactions of actin and myosin subfragment 1. Biochemistry. 1984; 23:4150–4155. [PubMed: 6487594]
8. Jancsó A, Graceffa P. Smooth muscle tropomyosin coiled-coil dimers. Subunit composition, assembly, and end-to-end interaction. J Biol Chem. 1991; 266:5891–5897. [PubMed: 2005125]
9. Lehrer SS, Golitsina NL, Geeves MA. Actin-tropomyosin activation of myosin subfragment 1 ATPase and thin filament cooperativity. The role of tropomyosin flexibility and end-to-end interactions. Biochemistry. 1997; 36:13449–13454. [PubMed: 9354612]
10. Smillie, LB. Biochemistry of Smooth Muscle Contraction. Barany, M., editor. Academic Press; San Diego: 1996. p. 63-75.
11. Chalovich JM. Actin mediated regulation of muscle contraction. Pharmacol Ther. 1992; 55:95–148. [PubMed: 1289901]

NIH-PA Author Manuscript

NIH-PA Author Manuscript

NIH-PA Author Manuscript

12. Wang CL. Caldesmon and the regulation of cytoskeletal functions. Adv Exp Med Biol. 2008; 644:250–272. [PubMed: 19209827]
13. Ngai PK, Walsh MP. Properties of caldesmon isolated from chicken gizzard. Biochem J. 1985; 230:695–707. [PubMed: 2998332]
14. Smith CWJ, Pritchard K, Marston SB. The mechanism of Ca2+ regulation of vascular smooth muscle thin filaments by caldesmon and calmodulin. J Biol Chem. 1987; 262:116–122. [PubMed: 2947901]
15. Velaz L, Hemric ME, Benson CE, Chalovich JM. The binding of caldesmon to actin and its effect on the ATPase activity of soluble myosin subfragments in the presence and absence of tropomyosin. J Biol Chem. 1989; 264:9602–9610. [PubMed: 2524487]
16. Chalovich JM, Cornelius P, Benson CE. Caldesmon inhibits skeletal actomyosin subfragment-1 ATPase activity and the binding of myosin subfragment-1 to actin. J Biol Chem. 1987; 262:5711–5716. [PubMed: 2952642]
17. Sen A, Chen YD, Yan B, Chalovich JM. Caldesmon reduces the apparent rate of binding of myosin S1 to actin- tropomyosin. Biochemistry. 2001; 40:5757–5764. [PubMed: 11341841]
18. Sen A, Chalovich JM. Caldesmon-actin-tropomyosin contains two types of binding sites for myosin S1. Biochemistry. 1998; 37:7526–7531. [PubMed: 9585567]
19. Kraft T, Chalovich JM, Yu LC, Brenner B. Parallel inhibition of active force and relaxed fiber stiffness by caldesmon fragments at physiological ionic strength and temperature conditions: Additional evidence that weak cross- bridge binding to actin is an essential intermediate for force generation. Biophys J. 1995; 68:2404–2418. [PubMed: 7647245]
20. Fredricksen S, Cai A, Gafurov B, Resetar A, Chalovich JM. Influence of ionic strength, actin state, and caldesmon construct size on the number of actin monomers in a caldesmon binding site. Biochemistry. 2003; 42:6136–6148. [PubMed: 12755616]
21. Marston SB, Redwood CS. The essential role of tropomyosin in cooperative regulation of smooth muscle thin filament activity by caldesmon. J Biol Chem. 1993; 268:12317–12320. [PubMed: 8509369]
22. Ansari S, Alahyan M, Marston SB, El Mezgueldi M. Role of Caldesmon in the Ca2+ Regulation of Smooth Muscle Thin Filaments: evidence for a cooperative switching mechanism. J Biol Chem. 2008; 283:47–56. [PubMed: 17933868]
23. Hodgkinson JL, Marston SB, Craig R, Vibert P, Lehman W. Three-dimensional image reconstruction of reconstituted smooth muscle thin filaments: Effects of caldesmon. Biophys J. 1997; 72:2398–2404. [PubMed: 9168017]
24. Borrego-Diaz E, Chalovich JM. Kinetics of regulated actin transitions measured by probes on tropomyosin. Biophys J. 2010; 98:2601–2609. [PubMed: 20513404]
25. Hill TL, Eisenberg E, Chalovich JM. Theoretical models for cooperative steady-state ATPase activity of myosin subfragment-1 on regulated actin. Biophys J. 1981; 35:99–112. [PubMed: 6455170]
26. McKillop DFA, Geeves MA. Regulation of the interaction between actin and myosin subfragment 1: Evidence for three states of the thin filament. Biophys J. 1993; 65:693–701. [PubMed: 8218897]
27. Chalovich JM. Regulation of striated muscle contraction: a discussion. J Muscle Res Cell Motil. 2002; 23:353–361. [PubMed: 12630710]
28. Spudich JA, Watt S. The regulation of rabbit skeletal muscle contraction. I Biochemical studies of the interaction of the tropomyosin-troponin complex with actin and the proteolytic fragments of myosin. J Biol Chem. 1971; 246:4866–4871. [PubMed: 4254541]
29. Eisenberg E, Kielley WW. Troponin-tropomyosin complex. Column chromatographic separation and activity of the three active troponin components with and without tropomyosin present. J Biol Chem. 1974; 249:4742–4748. [PubMed: 4276966]
30. Kielley WW, Harrington WF. A model for the myosin molecule. Biochim Biophys Acta. 1960; 41:401–421. [PubMed: 14408979]
31. Weeds AG, Taylor RS. Separation of subfragment-1 isozymes from rabbit skeletal muscle myosin. Nature. 1975; 257:54–56. [PubMed: 125854]

NIH-PA Author Manuscript

NIH-PA Author Manuscript

NIH-PA Author Manuscript

32. Bretscher A. Smooth Muscle Caldesmon: rapid purification and F-actin cross-linking properties. J Biol Chem. 1984; 259:12873–12880. [PubMed: 6092349]
33. Hibbs RE, Talley TT, Taylor P. Acrylodan-conjugated Cysteine Side Chains Reveal Conformational State and Ligand Site Locations of the Acetylcholine-binding Protein. J Biol Chem. 2004; 279:28483–28491. [PubMed: 15117947]
34. Chalovich JM, Chen Y, Dudek R, Luo H. Kinetics of binding of caldesmon to actin. J Biol Chem. 1995; 270:9911–9916. [PubMed: 7730374]
35. Chalovich JM, Eisenberg E. Inhibition of actomyosin ATPase activity by troponin-tropomyosin without blocking the binding of myosin to actin. J Biol Chem. 1982; 257:2432–2437. [PubMed: 6460759]
36. Williams DL Jr, Greene LE, Eisenberg E. Cooperative turning on of myosin subfragment 1 adenosine triphosphatase activity by the troponin-tropomyosin-actin complex. Biochemistry. 1988; 27:6987–6993. [PubMed: 2973810]
37. Lehman W, Hatch V, Korman V, Rosol M, Thomas L, Maytum R, Geeves MA, Van Eyk JE, Tobacman LS, Craig R. Tropomyosin and actin isoforms modulate the localization of tropomyosin strands on actin filaments. J Mol Biol. 2000; 302:593–606. [PubMed: 10986121]
38. Hemric ME, Chalovich JM. Effect of caldesmon on the ATPase activity and the binding of smooth and skeletal myosin subfragments to actin. J Biol Chem. 1988; 263:1878–1885. [PubMed: 2962997]
39. Pirani A, Xu C, Hatch V, Craig R, Tobacman LS, Lehman W. Single particle analysis of relaxed and activated muscle thin filaments. J Mol Biol. 2005:761–772. [PubMed: 15713461]
40. Alahyan M, Webb MR, Marston SB, El Mezgueldi M. The mechanism of smooth muscle caldesmon-tropomyosin inhibition of the elementary steps of the actomyosin ATPase. J Biol Chem. 2006:19433–19448. [PubMed: 16540476]
41. Chalovich JM, Sen A, Resetar A, Leinweber B, Fredricksen RS, Lu F, Chen YD. Caldesmon: binding to actin and myosin and effects on elementary steps in the ATPase cycle. Acta Physiol Scand. 1998; 164:427–435. [PubMed: 9887966]

NIH-PA Author Manuscript
NIH-PA Author Manuscript
NIH-PA Author Manuscript

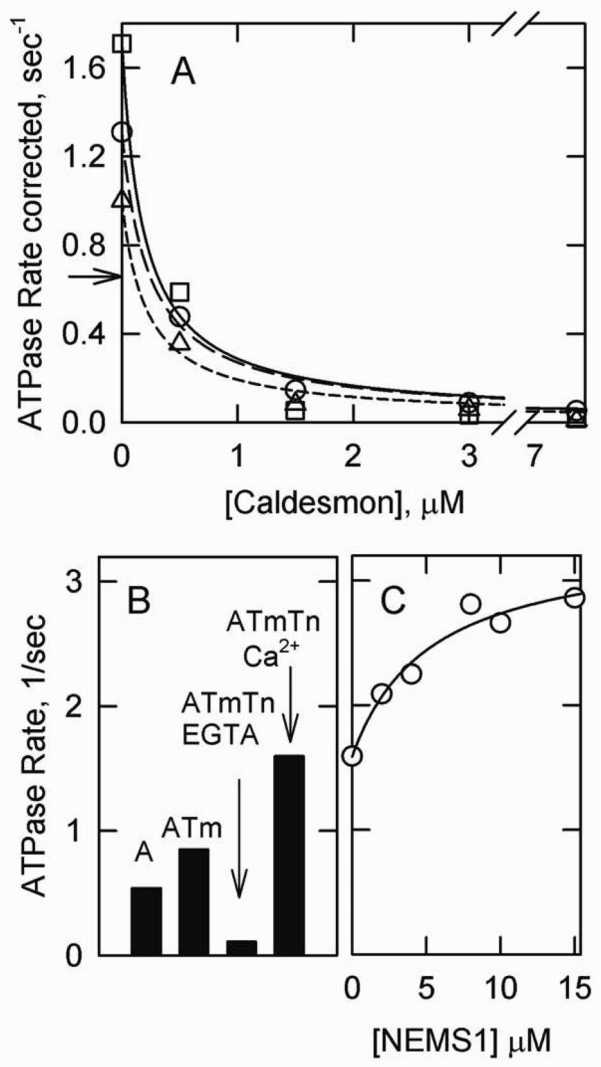

Figure 1.

Regulation of actin activated S1 ATPase activity by smooth muscle tropomyosin. A. Dependence of the rate on the caldesmon concentration in the presence of unlabeled tropomyosin (squares), acrylodan labeled tropomyosin (circles) and pyrene labeled tropomyosin (triangles). The arrow shows the rate of ATPase activity in the absence of tropomyosin and caldesmon. B. ATPase rates in the presence of actin (A), actin and acrylodan tropomyosin (ATm), actin, acrylodan tropomyosin, skeletal troponin and no calcium (ATmTn EGTA) and actin, tropomyosin, troponin and calcium (ATmTn Ca^{2+}). C. Effect of increasing concentrations of NEM-S1 on ATPase activity in the presence of actin, acrylodan labeled smooth tropomyosin, skeletal troponin and saturating calcium. Conditions: 0.3 μM S1, 10 μM actin, 3.5 μM tropomyosin, 4.3 μM troponin or 0.5–7.5 μM caldesmon in a buffer containing 2 mM ATP, 4.8 mM $MgCl_2$, 35.8 mM NaCl, 10 mM MOPS, 0.5 mM dithiothreitol, 1 mM EGTA or 0.5 mM $CaCl_2$, pH 7 and 25° C.

NIH-PA Author Manuscript
NIH-PA Author Manuscript
NIH-PA Author Manuscript

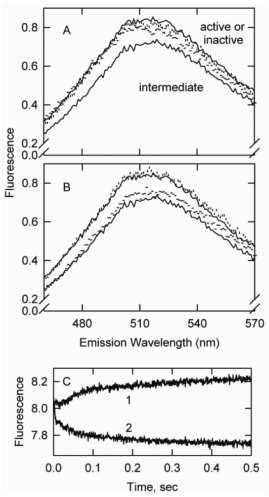

Figure 2.

Fluorescence emission spectra of acrylodan labeled smooth muscle tropomyosin bound to actin. A. Actin-tropomyosin alone (lower solid curve), with troponin (horizontal bars), with troponin and S1 (vertical bars) and with S1 and no troponin (upper solid curve). B. Actin-tropomyosin alone (lower solid curve), with caldesmon (horizontal bars), with caldesmon and S1 (vertical bars) and with S1 and no caldesmon (upper solid curve). Conditions: 154 mM KCl, 20 mM MOPS pH 7, 2 mM EGTA, 2 mM $MgCl_2$, 1 mM dithiothreitol at 15° C. Protein concentrations used were 2 μM actin, 0.86 μM acrylodan labeled tropomyosin, 0.86 μM skeletal muscle troponin, 0.86 μM caldesmon, and 2 μM S1. C. Effect of Ca^{2+} on acrylodan-tropomyosin fluorescence in the presence of skeletal troponin. Curve 1 shows the effect of rapidly lowering $[Ca^{2+}]_{free}$ by actin-tropomyosin-troponin containing 0.2 mM $CaCl_2$ with buffer containing 2 mM EGTA. Curve 2 shows the effect of rapidly increasing $[Ca^{2+}]_{free}$ by mixing actin-tropomyosin-troponin containing 1 mM EGTA with buffer containing 1.2 mM $CaCl_2$. Curves 1 and 2 were at 2.8 °C.

NIH-PA Author Manuscript

NIH-PA Author Manuscript

NIH-PA Author Manuscript

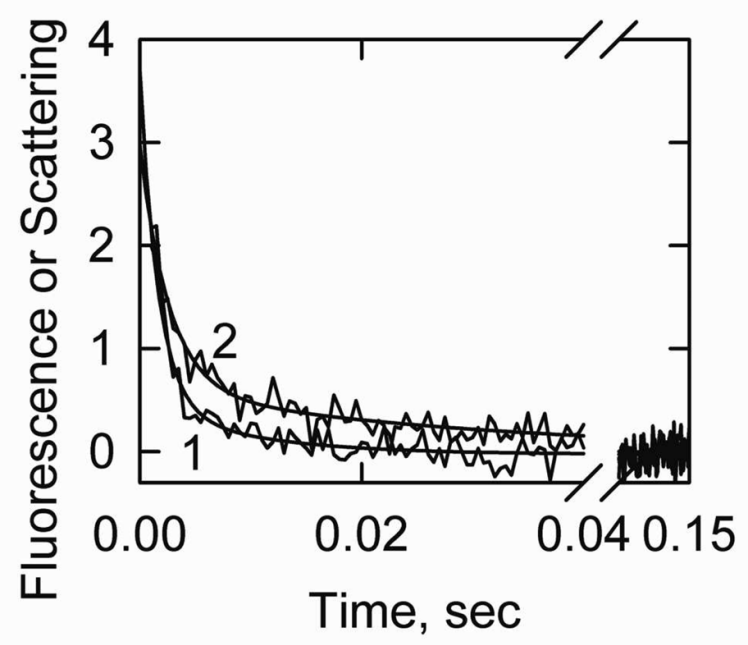

Figure 3.

S1-ATP dissociation experiment showing the transition from the active state to the intermediate state of actin-smooth muscle acrylodan tropomyosin. Final conditions: 2 μM actin, 0.86 μM acrylodan smooth muscle tropomyosin, 2 μM S1 at 5° C. The final buffer composition was 2 mM ATP, 6 mM $MgCl_2$, 142 mM KCl, 20 mM MOPS, 2 mM EGTA and 1 mM dithiothreitol, pH 7.0. Curve 1: light scattering, k_{app} (major phase) = 640 s^{-1} and shown fit to Model A was with k_{3A} = 700/sec. Curve 2: acrylodan fluorescence, k_{app} (major phase) = 400 s^{-1}. The simulated curve was created with Model A with k_{3a} = 700/sec and k_{5A} = 600/sec. Reverse rate constants were assumed to be zero.

NIH-PA Author Manuscript

NIH-PA Author Manuscript

NIH-PA Author Manuscript

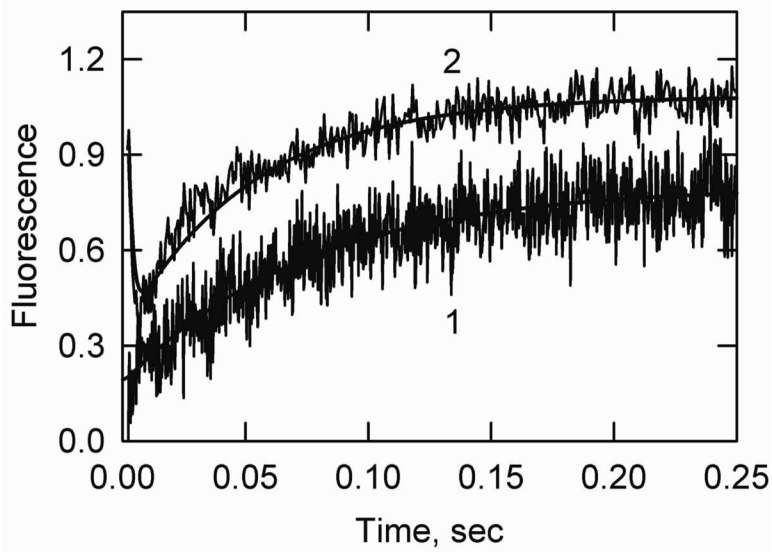

Figure 4.

S1-ATP dissociation experiment in the presence of troponin and absence of Ca^{2+}. Final conditions: 2 μM actin, 0.86 μM acrylodan smooth muscle tropomyosin, 0.86 μM skeletal troponin, 2 μM S1. The buffer composition was identical to that of Figure 3. Smooth curves are fits of Model Curve 1: 5° C, $k_{7A} + k_{8A} = 14$/sec. Curve 2: 3.5° C, $k_{3A} = 632$/sec, $k_{5A} = 1180$/sec, $k_{7A} + k_{8A} = 13$/sec. Binding to ATP was assumed to be instantaneous; reverse rate constants not listed were set to zero for the simulation with Model A. Exponential fits to the same curves gave $k_{app} = 14$/sec for curve 1 and $k_{app1} = 786$/sec and $k_{app2} = 20$/sec for curve 2.

NIH-PA Author Manuscript

NIH-PA Author Manuscript

NIH-PA Author Manuscript

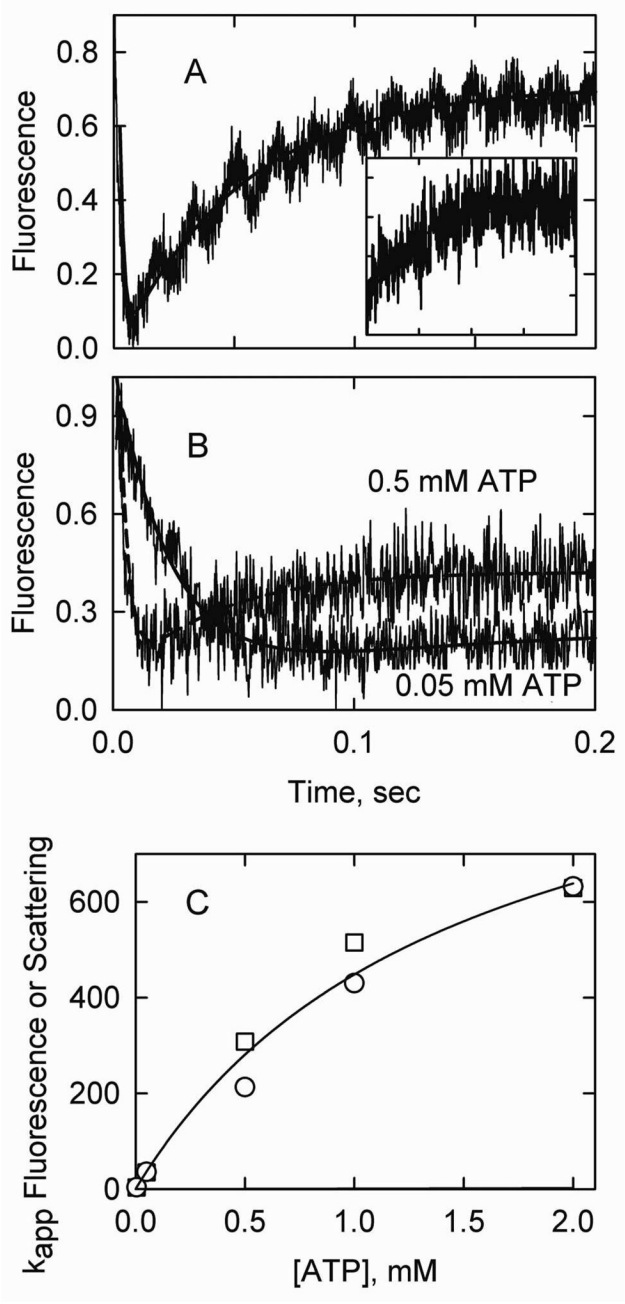

Figure 5.

S1-ATP dissociation experiments in the presence of caldesmon. Final conditions: 2 μM actin, 0.86 μM acrylodan smooth muscle tropomyosin, 0.86 μM caldesmon, 2 μM S1, 5° C and the same buffer as in Figure 3. Solid curves are fits to Model A. A. Acrylodan-tropomyosin fluorescence following S1-ATP detachment with k_{5A} = 1560/sec and k_{7A} + k_{8A} =19/sec. An exponential fit gave k_{app1} = 504/sec and k_{app2} = 19/sec. The inset shows an S1-ATP dissociation experiment with 0.5 μM S1 with k_{5A} = 2109/sec and k_{7A} + k_{8A} = 21/sec. B. Fluorescence transients for experiments with 0.5 mM and 0.05 mM ATP but with the ionic strength adjusted with KCl. For 0.5 mM ATP, k_{3A}= 281/sec, k_{5A} = 1030/sec, k_{7A} + k_{8A} = 25/sec. An exponential fit gave k_{app1} = 237/sec and k_{app2} =23/sec for 0.5 mM ATP

and k_{app} = 43/sec for 0.05 mM ATP. C. Apparent rate constants (exponential fits) for light scattering (squares) and acrylodan fluorescence (circles) as a function of [ATP].

NIH-PA Author Manuscript
NIH-PA Author Manuscript
NIH-PA Author Manuscript

NIH-PA Author Manuscript
NIH-PA Author Manuscript
NIH-PA Author Manuscript

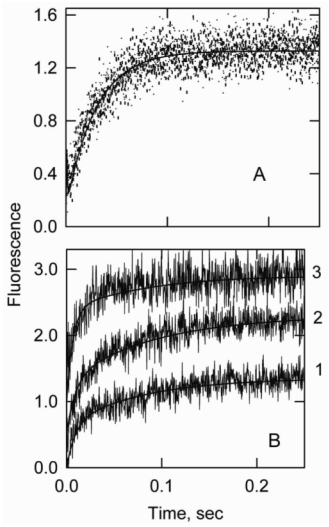

Figure 6.

Caldesmon binding to actin-tropomyosin. A. NBD-caldesmon binding to actin-tropomyosin (dots, k_{app} = 30.9/sec) and result of rapid S1-ATP dissociation from S1-actin-tropomyosin-NBD-caldesmon (vertical bars, k_{app} = 30.8/sec). The theoretical curve was produced from Model B with the following parameters: k_{1B} = 43 $\mu M^{-1}s^{-1}$, k_{2B} = 47/sec, k_{3B} = 30/sec, k_{4B} = 3.3/sec. The buffer was the same as in Figure 3 with 2 μM actin, 0.43 μM unlabeled tropomyosin, 0.6 μM caldesmon. The S1-ATP dissociation experiment (vertical bars) also contained 2 μM S1 and 2 mM ATP. B. Caldesmon binding to acrylodan tropomyosin-actin at several caldesmon concentrations. The buffer composition was the same as in Figure 3 with 2 μM actin, 0.86 μM acrylodan labeled tropomyosin and either 0.6 (curve 1), 1.2 (curve 2) or 2 (curve 3) μM caldesmon. Data were collected at 5° C. Fits of Model B to the data are shown as smooth curves. Values of k_{1B} were 14, 12 and 24$\mu M^{-1}s^{-1}$ for 0.6, 1.2 and 2 μM caldesmon, respectively. Other values were k_{2B} = 47/sec, k_{3B} =38/sec, k_{4B} = 4/sec.

NIH-PA Author Manuscript

NIH-PA Author Manuscript

NIH-PA Author Manuscript

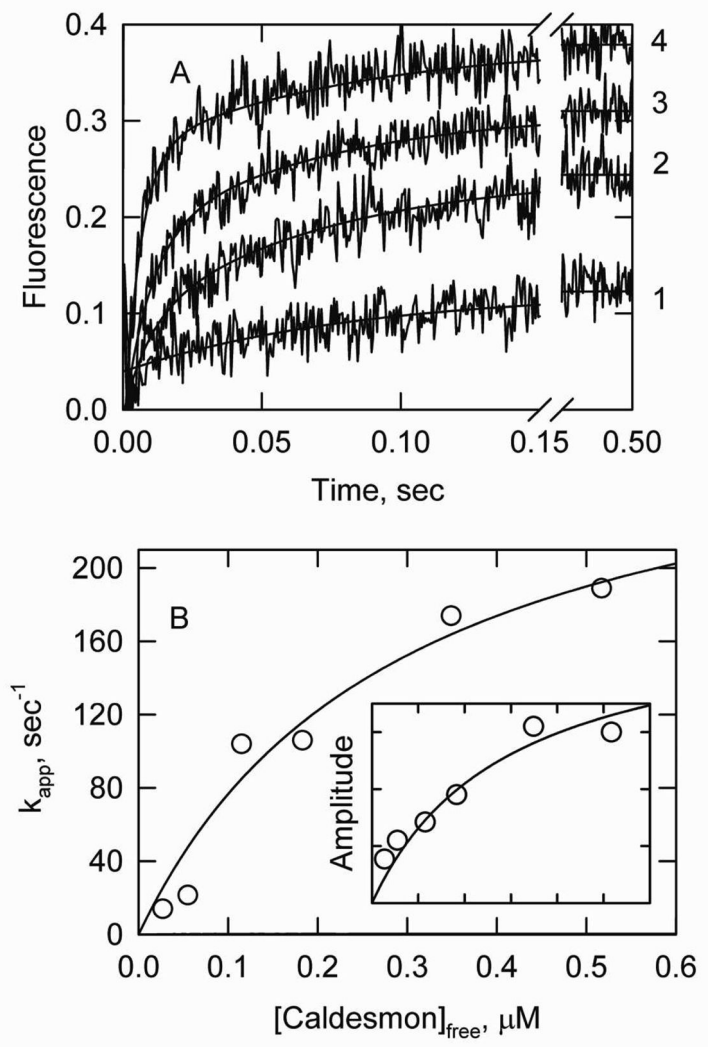

Figure 7.

S1-ATP dissociation experiments with variable caldesmon concentrations at low ionic strength. The S1-ATP dissociation study was done at 2.7° C in a buffer containing 25 mM NaCl, 8 mM MOPS, 4.7 mM $MgCl_2$, 0.25 mM EGTA and 2 mM ATP, pH 7.0. A. Curves 1 through 4 are time courses of fluorescence changes at total caldesmon concentrations of 0.1, 0.28, 0.38 and 0.57 μM, respectively. Solid lines are fits of a biexponential model to the curves. B. Dependence of the apparent rate constant for the major (faster) transition as a function of the calculated free caldesmon concentration. The inset shows amplitudes of the major transition as a function of free caldesmon on the same scale. Both curves were fit to a binding equation with half of the maximum signal occurring at 0.29 μM free caldesmon.